Preprints of the 21st IFAC World Congress (Virtual)
Berlin, Germany, July 12-17, 2020

Multivariable Adaptive Dual Layer Super-Twisting Algorithm ⋆

Azevedo Filho, Jair L. * **Nunes, Eduardo V. L.** *

* *COPPE-Federal University of Rio de Janeiro, Rio de Janeiro, RJ, 21941-901, Brazil (e-mail: jair.azevedo@ufrj.br; eduardo@coep.ufrj.br).*

Abstract: In this paper, a novel Multivariable Adaptive Super-Twisting Algorithm is proposed. The adaptation scheme is based on a dual-layer structure and does not require the knowledge of upper bounds for the matched disturbances. By exploiting information extracted from the equivalent control, it is possible to adapt both gains to enforce a second-order sliding mode while avoiding a conservative overestimation of the disturbance, which is important to mitigate the undesirable effects of chattering.

Keywords: Sliding mode control, Lyapunov methods, higher-order sliding modes, multivariable control, disturbance rejection, nonlinear adaptive control.

1. INTRODUCTION

Sliding Mode Control is a powerful method for robust control of uncertain systems subject to matched disturbances. One main obstacle for its practical implementation is the appearance of undesirable oscillations caused by the high-frequency switching control action. This phenomenon is referred to as chattering and can lead to a system performance degradation (Utkin, 1992; Shtessel et al., 2014).

Although several techniques were already available for chattering attenuation, the introduction of controllers based on the so-called higher-order sliding modes (HOSM) (Levant, 1993) seemed a breakthrough, since this innovative approach preserves the main sliding-mode features, and also can eliminate chattering under ideal situations. However, in real systems, non-idealities are always present, and consequentially this approach can only mitigate the chattering effect (Boiko and Fridman, 2005).

Among all second-order sliding mode approaches, the Super-Twisting Algorithm (STA) gained considerable attention from the SMC community due to its distinctive advantage of not requiring the sliding variable derivative to be implemented (Levant, 2003). Recently, the useful Lyapunov function approach introduced by (Moreno and Osorio, 2008) has stirred new developments for the STA with particular interest to adaptive schemes.

Several authors considered adaptive laws to increase the gains of the STA so as to ensure the realization of second-order sliding modes (Plestan et al., 2010; Shtessel et al., 2012; Alwi and Edwards, 2013; Bartolini et al., 2013). However, in these works, the gains are non-decreasing, resulting in some conservatism, which in turn can compound the chattering problem. To address this issue, (Utkin and Poznyak, 2013) proposed an adaptive scheme that uses information about the disturbance/uncertainty extracted from the equivalent control to enforce the sliding motion while reducing the control action magnitude. However, in this approach, only one gain is adapted while the other is assumed sufficiently large.

Following in the same direction, (Edwards and Shtessel, 2016) proposed a modification to the usual super-twisting algorithm structure together with the use of a dual-layer adaptive scheme allowing the adaptation of both gains. The adaptive scheme is also based on the knowledge of the equivalent control and tries to obtain the minimum possible values for the gains preserving the sliding mode. However, as in (Utkin and Poznyak, 2013), the scheme proposed in (Edwards and Shtessel, 2016) was also restricted to SISO systems.

In (Zhao et al., 2019), a fault-tolerant control strategy is developed to achieve a finite-time and precise attitude tracking for rigid spacecraft. A double-layer adaptive algorithm based on equivalent control is proposed combined with a multivariable super-twisting algorithm. However, as in (Utkin and Poznyak, 2013), the proposed strategy adapts only one gain, and the other is set sufficiently large.

The main contribution of this paper is to propose a new multivariable non-decoupled super-twisting algorithm with adaptive gains. Although a generalized formalism is used to present the algorithm, the detailed development is restricted to a particular case closer to the SISO version proposed in (Edwards and Shtessel, 2016). To facilitate a possible generalization for a class of super-twisting-like algorithms, we introduce an additional parameter in the dual-layer adaptive scheme. Both gains are adapted using information extracted from the equivalent control so as to sustain the sliding motion while avoiding a conservative overestimation for their values, mitigating the chattering problem. Global finite-time convergence is guaranteed by a Lyapunov approach. The proposed method is applied to the problem of the detection and reconstruction of cyber-attacks in a bus power system. The theoretical findings are illustrated by numerical simulations.

Preliminaries: The euclidean norm of a vector $\boldsymbol{y}$ and the corresponding induced norm of a matrix $\boldsymbol{A}$ are denoted by

⋆ This work was supported in part by CAPES, CNPq, and FAPERJ.

$||\boldsymbol{y}||$ and $||\boldsymbol{A}||$, respectively. The maximum and minimum eigenvalues of a matrix $\boldsymbol{A}$ are denoted by $\lambda_{max}(\boldsymbol{A})$ and $\lambda_{min}(\boldsymbol{A})$, respectively. Consider that $\boldsymbol{A}$, $\boldsymbol{B}$, $\boldsymbol{C}$, and $\boldsymbol{D}$ are matrices with compatible dimensions. Therefore from (Bernstein, 2009) the following Kronecker properties hold:

(P1). $(\boldsymbol{A}\otimes\boldsymbol{B})(\boldsymbol{C}\otimes\boldsymbol{D})=\boldsymbol{AC}\otimes\boldsymbol{BD}$
(P2). $\boldsymbol{A}\otimes\boldsymbol{C}+\boldsymbol{B}\otimes\boldsymbol{C}=(\boldsymbol{A}+\boldsymbol{B})\otimes\boldsymbol{C}$
(P3). $(\boldsymbol{A}\otimes\boldsymbol{B})^T=\boldsymbol{A}^T\otimes\boldsymbol{B}^T$

Here, Fillipov's definition for the solutions of discontinuous differential equations is assumed (Filippov, 1964).

2. MULTIVARIABLE ADAPTIVE SUPER-TWISTING ALGORITHM (MASTA)

Consider the following multivariable algorithm based on a variation of the Super-Twisting Algorithm:

$$\begin{aligned}\dot{\boldsymbol{\sigma}}(t)&=-\alpha(t)\boldsymbol{\phi}_1(\boldsymbol{\sigma})+\boldsymbol{\Phi}(t,\boldsymbol{\phi}_1)+\boldsymbol{z}(t)\\ \dot{\boldsymbol{z}}(t)&=-\beta(t)\boldsymbol{\phi}_2(\boldsymbol{\sigma})+\boldsymbol{d}(\boldsymbol{\sigma},t),\end{aligned}\tag{1}$$

$$\begin{aligned}&\alpha(t)=\alpha_0\sqrt{L(t)},\ \beta(t)=\beta_0L(t),\\ &\boldsymbol{\Phi}(t,\boldsymbol{\phi}_1)=-\frac{\dot{L}}{2L}\left(\frac{d\boldsymbol{\phi}_1}{d\boldsymbol{\sigma}}\right)^{-1}\boldsymbol{\phi}_1(\boldsymbol{\sigma}),\end{aligned}\tag{2}$$

where $\boldsymbol{\sigma}(t),\boldsymbol{z}(t)\in\mathbb{R}^n$ are the sliding variables, $L(t)\in\mathbb{R}$ is an adaptive gain to be defined later, α_0 and β_0 are positive constants and $\boldsymbol{d}(\boldsymbol{\sigma},t)\in\mathbb{R}^n$ is an input disturbance. The functions $\boldsymbol{\phi}_1(\boldsymbol{\sigma})$ and $\boldsymbol{\phi}_2(\boldsymbol{\sigma})$ are defined such that the following property holds

$$\boldsymbol{\phi}_2(\boldsymbol{\sigma})=\frac{d\boldsymbol{\phi}_1}{d\boldsymbol{\sigma}}\boldsymbol{\phi}_1(\boldsymbol{\sigma}),\quad\forall\boldsymbol{\sigma}(t)\neq\boldsymbol{0}\tag{3}$$

In order to closely represent a multivariable version of the algorithm proposed in (Edwards and Shtessel, 2016), these functions are chosen as

$$\boldsymbol{\phi}_1(\boldsymbol{\sigma})=\frac{\boldsymbol{\sigma}}{||\boldsymbol{\sigma}||^{\frac{1}{2}}},\quad\boldsymbol{\phi}_2(\boldsymbol{\sigma})=\frac{1}{2}\frac{\boldsymbol{\sigma}}{||\boldsymbol{\sigma}||}\tag{4}$$

In this case, the jacobian matrix $\boldsymbol{\phi_1'}(\boldsymbol{\sigma})\in\mathbb{R}^{n\times n}$ is given by

$$\boldsymbol{\phi_1'}(\boldsymbol{\sigma})=\frac{d\boldsymbol{\phi}_1(\boldsymbol{\sigma})}{d\boldsymbol{\sigma}}=\frac{1}{||\boldsymbol{\sigma}||^{\frac{1}{2}}}I_n-\frac{\boldsymbol{\sigma}\boldsymbol{\sigma}^T}{2||\boldsymbol{\sigma}||^{\frac{5}{2}}}\tag{5}$$

Furthermore, the quadratic form associated with $\boldsymbol{\phi_1'}(\boldsymbol{\sigma})$ is given by

$$\boldsymbol{v}^T\frac{d\boldsymbol{\phi}_1(\boldsymbol{\sigma})}{d\boldsymbol{\sigma}}\boldsymbol{v}=\frac{||\boldsymbol{v}||^2}{||\boldsymbol{\sigma}||^{\frac{1}{2}}}-\frac{\left(\boldsymbol{v}^T\boldsymbol{\sigma}\right)^2}{2||\boldsymbol{\sigma}||^{\frac{5}{2}}}\tag{6}$$

where, for every $\boldsymbol{\sigma}(t)\neq\boldsymbol{0}$, the minimum value is reached at the maximum value of $\boldsymbol{v}^T\boldsymbol{\sigma}$. From the Cauchy-Schwarz inequality for inner products, one has that $\boldsymbol{v}^T\boldsymbol{\sigma}\leq||\boldsymbol{v}||\cdot||\boldsymbol{\sigma}||$. Therefore, the following property holds for $n\geq2$

$$\boldsymbol{v}^T\boldsymbol{\phi_1'}(\boldsymbol{\sigma})\boldsymbol{v}\geq\lambda_{min}\left(\boldsymbol{\phi_1'}(\boldsymbol{\sigma})\right)||\boldsymbol{v}||^2,\quad\forall\,\boldsymbol{v}\in\mathbb{R}^n\tag{7}$$

$$\lambda_{min}\left(\boldsymbol{\phi_1'}(\boldsymbol{\sigma})\right)=\frac{1}{2||\boldsymbol{\sigma}(t)||^{\frac{1}{2}}}.\tag{8}$$

Therefore, $\forall\boldsymbol{\sigma}(t)\neq\boldsymbol{0}$, $\boldsymbol{\phi_1'}(\boldsymbol{\sigma})$ is a Symmetric and Positive Definite (S.P.D.) matrix. The equality in (7) holds when $\boldsymbol{v}$ is linearly dependent of $\boldsymbol{\sigma}$. The maximum value of the quadratic form occurs when $\boldsymbol{v}$ is orthogonal to $\boldsymbol{\sigma}$, i.e., $\boldsymbol{\sigma}^T\boldsymbol{v}=0$. Thus, the following inequality is satisfied for every $\boldsymbol{\sigma}(t)\neq\boldsymbol{0}$

$$\boldsymbol{v}^T\boldsymbol{\phi_1'}(\boldsymbol{\sigma})\boldsymbol{v}\leq\lambda_{max}\left(\boldsymbol{\phi_1'}(\boldsymbol{\sigma})\right)||\boldsymbol{v}||^2,\quad\forall\,\boldsymbol{v}\in\mathbb{R}^n\tag{9}$$

$$||\boldsymbol{\phi_1'}(\boldsymbol{\sigma})||=\lambda_{max}\left(\boldsymbol{\phi_1'}(\boldsymbol{\sigma})\right)=\frac{1}{||\boldsymbol{\sigma}(t)||^{\frac{1}{2}}}.\tag{10}$$

Note that, for $n=1$ and for every $\sigma\neq0$, $\phi_1'(\sigma)=\frac{1}{|\sigma|^{\frac{1}{2}}}$ is a scalar. From (4) and (8), it can be verified that

$$\boldsymbol{\phi}_2(\boldsymbol{\sigma})=\lambda_{min}\left(\boldsymbol{\phi_1'}(\boldsymbol{\sigma})\right)\boldsymbol{\phi}_1(\boldsymbol{\sigma}),\forall\boldsymbol{\sigma}(t)\neq\boldsymbol{0}\tag{11}$$

It is worth noting that properties (3), (7), (9) and (11) hold for other variations of the Super-Twisting algorithm, as can be seen in (Vidal et al., 2017). Thus, it seems that the results obtained here may be extended to a generalized class of Multivariable Super-Twisting based algorithms.

The strategy proposed here is divided into two parts: First, we show that, if $L(t)>||\boldsymbol{d}(\boldsymbol{\sigma},t)||$, then the sliding mode is achieved with a proper choice of α_0 and β_0. Thus, for the time being, we consider the following assumption:

Assumption 1: The function $L(t)$ is differentiable and satisfies $L(t)>max(||\boldsymbol{d}(\boldsymbol{\sigma},t)||,l_0),\forall t$, where $l_0>0\in\mathbb{R}$.

Later on, we consider an adaptation law to guarantee that Assumption 1 is satisfied and also to ensure non-overestimated values for the gains.

The stability properties of the proposed multivariable version of the STA are stated in the following Theorem.

Theorem 1. Consider the system (1) and suppose that Assumption 1 holds. Then, a second order sliding mode occurs making $\dot{\boldsymbol{\sigma}}=\boldsymbol{\sigma}=\boldsymbol{0}$ in finite time if the gains α_0 and β_0 are chosen such that

$$\frac{\alpha_0^2\beta_0^2}{\alpha_0^2+\beta_0+2}>\frac{\kappa^2}{\kappa-1},\tag{12}$$

where $\kappa>1$ is a design parameter.

Proof. Consider the following Lyapunov function candidate for the system (1):

$$V(t,\boldsymbol{\sigma},\boldsymbol{z})=p_1||\boldsymbol{\sigma}||L(t)-2p_2\frac{\boldsymbol{\sigma}^T\boldsymbol{z}}{||\boldsymbol{\sigma}||^{\frac{1}{2}}}L(t)^{\frac{1}{2}}+p_3||\boldsymbol{z}||^2\tag{13}$$

where p_1, p_2 and p_3 are positive constants which ensures that the symmetric matrix

$$\boldsymbol{P}=\begin{bmatrix}p_1&-p_2\\-p_2&p_3\end{bmatrix}>\boldsymbol{0}.$$

Now, considering the following notation

$$\boldsymbol{\zeta}=\begin{bmatrix}\boldsymbol{\zeta}_1^T&\boldsymbol{\zeta}_2^T\end{bmatrix}^T=\begin{bmatrix}\frac{\boldsymbol{\sigma}^T\sqrt{L(t)}}{||\boldsymbol{\sigma}||^{\frac{1}{2}}}&\boldsymbol{z}^T\end{bmatrix}^T\tag{14}$$

the Lyapunov function (13) can be rewritten as

$$V=\boldsymbol{\zeta}^T\boldsymbol{P_n}\boldsymbol{\zeta},\quad\boldsymbol{P_n}=\boldsymbol{P}\otimes\boldsymbol{I_n}\tag{15}$$

Since $L(t)>0$, and $\boldsymbol{P_n}=\boldsymbol{P}_n^T>0$, it follows that $V(t,\boldsymbol{\sigma},\boldsymbol{z})$ is a positive definite, continuous and radially unbounded function with respect to $(\boldsymbol{\sigma},\boldsymbol{z})$, and its derivative can be described in terms of $\dot{\boldsymbol{\zeta}}$ as follows

$$\dot{V} = \boldsymbol{\zeta}^T \boldsymbol{P_n} \dot{\boldsymbol{\zeta}} + \dot{\boldsymbol{\zeta}}^T \boldsymbol{P_n} \boldsymbol{\zeta} \tag{16}$$

From (1), on subspace $S = \{(\boldsymbol{\sigma}, \boldsymbol{v}) \in \Re^{2n} | \boldsymbol{\sigma} \neq \boldsymbol{0}\}$ it follows that:

$$\dot{\boldsymbol{\zeta}}_1 = \frac{\dot{L}}{2\sqrt{L}} \boldsymbol{\phi}_1 + \sqrt{L} \boldsymbol{\phi_1'}(\boldsymbol{\sigma}) \dot{\boldsymbol{\sigma}}$$

$$\dot{\boldsymbol{\zeta}}_1 = \frac{\dot{L}}{2\sqrt{L}} \boldsymbol{\phi}_1 + \sqrt{L} \boldsymbol{\phi_1'}(\boldsymbol{\sigma}) \left(-\alpha \boldsymbol{\phi}_1 + \boldsymbol{z} + \boldsymbol{\Phi}\right)$$

$$\dot{\boldsymbol{\zeta}}_1 = \left(\frac{\dot{L}}{2\sqrt{L}} \boldsymbol{\phi}_1 + \sqrt{L} \boldsymbol{\phi_1'}(\boldsymbol{\sigma}) \boldsymbol{\Phi}\right) + \sqrt{L} \boldsymbol{\phi_1'}(\boldsymbol{\sigma}) \left(-\alpha \boldsymbol{\phi}_1 + \boldsymbol{z}\right)$$

Selecting $\boldsymbol{\Phi}(t, \boldsymbol{\phi}_1)$ and $\alpha(t)$ as in (2), and using the notation proposed in (14), it follows that

$$\dot{\boldsymbol{\zeta}}_1 = \sqrt{L} \left(-\alpha_0 \boldsymbol{\phi_1'}(\boldsymbol{\sigma}) \zeta_1 + \frac{d\boldsymbol{\phi}_1}{d\boldsymbol{\sigma}} \zeta_2\right) \tag{17}$$

From (3), and (2), since $\boldsymbol{\zeta}_2(t) = \boldsymbol{z}(t)$, it can be verified

$$\dot{\boldsymbol{\zeta}}_2 = \sqrt{L} \left(-\beta_0 \boldsymbol{\phi_1'}(\boldsymbol{\sigma}) \boldsymbol{\phi}_1(\boldsymbol{\sigma}) \sqrt{L} + \frac{\boldsymbol{d}(\boldsymbol{\sigma}, t)}{\sqrt{L}}\right) \tag{18}$$

Rewriting (18), using (14), one has that

$$\dot{\boldsymbol{\zeta}}_2 = \sqrt{L} \left(-\beta_0 \boldsymbol{\phi_1'}(\boldsymbol{\sigma}) \zeta_1 + \boldsymbol{\Delta}\right) \tag{19}$$

where

$$\boldsymbol{\Delta} = \frac{\boldsymbol{d}(\boldsymbol{\sigma}, t)}{\sqrt{L}}. \tag{20}$$

Note that (17) and (19) can be written in a concise form

$$\dot{\boldsymbol{\zeta}} = \sqrt{L}(\bar{\boldsymbol{A}}_{\boldsymbol{0}} \boldsymbol{\zeta} + \bar{\boldsymbol{B}}_{\boldsymbol{0}} \boldsymbol{\Delta}) \tag{21}$$

where $\bar{\boldsymbol{A}}_{\boldsymbol{0}} = \boldsymbol{A_0} \otimes \boldsymbol{\phi_1'}(\boldsymbol{\sigma})$ and $\bar{\boldsymbol{B}}_{\boldsymbol{0}} = \boldsymbol{B_0} \otimes \boldsymbol{I_n}$ with

$$\boldsymbol{A_0} = \begin{bmatrix} -\alpha_0 & 1 \\ -\beta_0 & 0 \end{bmatrix}, \quad \boldsymbol{B_0} = \begin{bmatrix} 0 \\ 1 \end{bmatrix} \tag{22}$$

Rewriting (16) with (21), it follows that

$$\dot{V} = \sqrt{L} \left(\boldsymbol{\zeta}^T \left(\boldsymbol{P_n} \bar{\boldsymbol{A}}_{\boldsymbol{0}} + \bar{\boldsymbol{A}}_{\boldsymbol{0}}^{\boldsymbol{T}} \boldsymbol{P_n}\right) \boldsymbol{\zeta} + 2\boldsymbol{\zeta}^T \boldsymbol{P_n} \bar{\boldsymbol{B}}_{\boldsymbol{0}} \boldsymbol{\Delta}\right) \tag{23}$$

Defining $\bar{\boldsymbol{Q}} = \boldsymbol{P_n} \bar{\boldsymbol{A}}_{\boldsymbol{0}} + \bar{\boldsymbol{A}}_{\boldsymbol{0}}^{\boldsymbol{T}} \boldsymbol{P_n}$ and invoking the Kronecker properties (P1),(P2), and (P3), it can be shown that

$$\begin{aligned} \bar{\boldsymbol{Q}} &= (\boldsymbol{P A_0}) \otimes (\boldsymbol{I_n} \boldsymbol{\phi_1'}(\boldsymbol{\sigma})) + (\boldsymbol{A_0^T P}) \otimes (\boldsymbol{I_n} \boldsymbol{\phi_1'}(\boldsymbol{\sigma})) \\ \bar{\boldsymbol{Q}} &= \boldsymbol{Q} \otimes \boldsymbol{\phi_1'}(\boldsymbol{\sigma}), \end{aligned} \tag{24}$$

where $\boldsymbol{Q} = \boldsymbol{P A_0} + \boldsymbol{A_0^T P} \in \mathbb{R}^{2\times 2}$. To simplify the analysis, choosing $p_1 = -\alpha_0 p_2 + \beta_0 p_3$, it follows that

$$\boldsymbol{Q} = \begin{bmatrix} 2((\beta_0 + \alpha_0^2)p_2 - \alpha_0 \beta_0 p_3) & 0 \\ 0 & -2p_2 \end{bmatrix}$$

If $p3$ is chosen such that

$$p3 > \frac{\beta_0 + \alpha_0^2}{\alpha_0 \beta_0}, \tag{25}$$

then $\boldsymbol{Q}$ becomes negative definite. In this case, from (7), the quadratic term $\boldsymbol{\zeta}^T \bar{\boldsymbol{Q}} \boldsymbol{\zeta}$ can be upper bounded by

$$\begin{aligned} \boldsymbol{\zeta}^T \bar{\boldsymbol{Q}} \boldsymbol{\zeta} &\leq \frac{2((\beta_0 + \alpha_0^2)p_2 - \alpha_0 \beta_0 p_3)||\boldsymbol{\zeta}_1||^2 - 2p_2||\boldsymbol{\zeta}_2||^2}{2||\boldsymbol{\sigma}(t)||^{\frac{1}{2}}} \\ \boldsymbol{\zeta}^T \bar{\boldsymbol{Q}} \boldsymbol{\zeta} &\leq \frac{1}{2||\boldsymbol{\sigma}(t)||^{\frac{1}{2}}} \bar{\boldsymbol{\zeta}}^T \boldsymbol{Q} \bar{\boldsymbol{\zeta}} \end{aligned} \tag{26}$$

where $\bar{\boldsymbol{\zeta}}^T = [||\boldsymbol{\zeta}_1|| \quad ||\boldsymbol{\zeta_2}||]^T \in \mathbb{R}^2, \ \boldsymbol{Q} = \boldsymbol{Q}^T < 0.$

From (15), (20) and (21), the term $2\boldsymbol{\zeta}^T \boldsymbol{P_n} \bar{\boldsymbol{B}}_{\boldsymbol{0}} \boldsymbol{\Delta}$ can be upper bounded as

$$2\boldsymbol{\zeta}^T \boldsymbol{P_n} \bar{\boldsymbol{B}}_{\boldsymbol{0}} \boldsymbol{\Delta} \leq \frac{2p_2|\boldsymbol{\zeta}_1^T \boldsymbol{d}|}{\sqrt{L}} + \frac{2p_3|\boldsymbol{\zeta}_2^T \boldsymbol{d}|}{\sqrt{L}} \tag{27}$$

which can be further upper bounded by

$$2\boldsymbol{\zeta}^T \boldsymbol{P_n} \bar{\boldsymbol{B}}_{\boldsymbol{0}} \boldsymbol{\Delta} \leq \frac{1}{2||\boldsymbol{\sigma}||^{\frac{1}{2}}} \left(4p_2||\boldsymbol{\zeta}_1|| + 4p_3||\boldsymbol{\zeta}_2||\right) \frac{||\boldsymbol{\sigma}||^{\frac{1}{2}}||\boldsymbol{d}||}{\sqrt{L}}$$

From (14), $||\boldsymbol{\zeta}_1|| = \sqrt{L}||\boldsymbol{\sigma}||^{\frac{1}{2}}$, and since $L(t) > ||\boldsymbol{d}(\boldsymbol{\sigma}, t)||$, according to Assumption 1, it is possible to conclude that

$$2\boldsymbol{\zeta}^T \boldsymbol{P_n} \bar{\boldsymbol{B}}_{\boldsymbol{0}} \boldsymbol{\Delta} \leq \frac{1}{2||\boldsymbol{\sigma}||^{\frac{1}{2}}} \left(4p_2||\boldsymbol{\zeta}_1||^2 + 4p_3||\boldsymbol{\zeta}_2|| \, ||\boldsymbol{\zeta}_1||\right) \tag{28}$$

Using (26) and (28), the function $\dot{V}$ can be upper bounded as follows

$$\begin{aligned} \dot{V} \leq& -\frac{\sqrt{L}}{2||\boldsymbol{\sigma}(t)||^{\frac{1}{2}}} \left(\bar{\boldsymbol{\zeta}}^T \begin{bmatrix} 2(\alpha_0 \beta_0 p_3 - p_2(\alpha_0^2 + \beta_0 + 2)) & -2p_3 \\ -2p_3 & 2p_2 \end{bmatrix} \bar{\boldsymbol{\zeta}}\right) \\ =& -\frac{\sqrt{L}}{2||\boldsymbol{\sigma}(t)||^{\frac{1}{2}}} \left(\bar{\boldsymbol{\zeta}}^T \boldsymbol{W} \bar{\boldsymbol{\zeta}}\right) \end{aligned} \tag{29}$$

Note that by defining $p_3 = \frac{\kappa p_2}{\alpha_0 \beta_0}\left(\alpha_0^2 + \beta_0 + 2\right)$ and α_0 and β_0 satisfying (12), the matrix $\boldsymbol{W}$ becomes positive definite. In addition, this choice of p_3 also satisfies inequality (25). Therefore, on subspace $S = \{(\boldsymbol{\sigma}, \boldsymbol{z}) \in \Re^{2n} | \boldsymbol{\sigma} \neq \boldsymbol{0}\}$, $\dot{V}$ is negative definite, which ensures the boundedness of the sliding variables. From Rayleigh's inequality, it follows that $\lambda_{min}(\boldsymbol{W})||\bar{\boldsymbol{\zeta}}||^2 \leq \bar{\boldsymbol{\zeta}}^T \boldsymbol{W} \bar{\boldsymbol{\zeta}}$ and $V \leq \lambda_{max}(\boldsymbol{P_n})||\boldsymbol{\zeta}||^2 = \lambda_{max}(\boldsymbol{P_n})||\bar{\boldsymbol{\zeta}}||^2$. Thus, the function $\dot{V}$ can be upper bounded by

$$\dot{V} \leq -\sqrt{L} \frac{1}{2||\boldsymbol{\sigma}(t)||^{\frac{1}{2}}} \frac{\lambda_{min}(\boldsymbol{W})}{\lambda_{max}(\boldsymbol{P_n})} V \tag{30}$$

From (15) and since $||\boldsymbol{\zeta}|| \geq ||\boldsymbol{\zeta}_1|| = \sqrt{L}||\boldsymbol{\sigma}||^{\frac{1}{2}}$, it follows that $\sqrt{\lambda_{min}(\boldsymbol{P_n})}||\boldsymbol{\zeta}_1|| = \sqrt{\lambda_{min}(\boldsymbol{P_n})}\sqrt{L}||\boldsymbol{\sigma}||^{\frac{1}{2}} \leq \sqrt{V}$. Thus, from Assumption 1, the following result can be obtained

$$\dot{V} \leq -\frac{L}{2} \frac{\lambda_{min}(\boldsymbol{W})\sqrt{\lambda_{min}(\boldsymbol{P_n})}}{\lambda_{max}(\boldsymbol{P_n})} \sqrt{V} \leq -\kappa \sqrt{V}, \tag{31}$$

where $\kappa = \frac{l_0}{2} \frac{\lambda_{min}(\boldsymbol{W})\sqrt{\lambda_{min}(\boldsymbol{P_n})}}{\lambda_{max}(\boldsymbol{P_n})} > 0$ is a known constant.

Note that $V(t, \boldsymbol{\sigma}, \boldsymbol{z})$ defined in (13) is continuous and differentiable on the set $S = \{(\boldsymbol{\sigma}, \boldsymbol{z}) \in \Re^{2n} | \boldsymbol{\sigma} \neq \boldsymbol{0}\}$. On the complementary set $\bar{S} = \{(\boldsymbol{\sigma}, \boldsymbol{z}) \in \Re^{2n} | \boldsymbol{\sigma} = \boldsymbol{0}\}$, the trajectories of (1) cannot stay on $\bar{S}/\{\boldsymbol{0}\}$, since $\boldsymbol{z} \neq \boldsymbol{0} \implies \dot{\boldsymbol{\sigma}} \neq \boldsymbol{0}$. Thus, V is a continuously decreasing function and from the results obtained in (Deimling, 1992) for differential inclusions, the equilibrium point $(\boldsymbol{\sigma}, \boldsymbol{z}) = \boldsymbol{0}$ is reached in finite time. From (1), if $\boldsymbol{\sigma} = \boldsymbol{z} = 0$, then it can be verified that $\dot{\boldsymbol{\sigma}}(t) = 0$ in finite time.

To complete the analysis, we must ensure that Assumption 1 is valid. Therefore, the problem becomes selecting an appropriate adaptation law for $L(t)$. The adaptation considered here is a small variation of the one proposed in (Edwards and Shtessel, 2016), where the concept of equivalent control is considered, allowing $L(t)$ to be designed as a non-overestimated "upper-bound" function for $\boldsymbol{d}(\boldsymbol{\sigma}, t)$. To this end, the discontinuous signal $\frac{\beta(t)}{2} \frac{\boldsymbol{\sigma}(t)}{||\boldsymbol{\sigma}(t)||}$ is used. During the sliding mode, $\boldsymbol{\sigma} = \boldsymbol{0}$ and $\dot{\boldsymbol{\sigma}} = \boldsymbol{z} = \boldsymbol{0}$, which implies that

$$\left.\frac{\beta(t)}{2} \frac{\boldsymbol{\sigma}(t)}{||\boldsymbol{\sigma}(t)||}\right|_{eq} = \boldsymbol{d}(\boldsymbol{\sigma}, t) \tag{32}$$

where $\left.\frac{\beta(t)}{2} \frac{\boldsymbol{\sigma}(t)}{||\boldsymbol{\sigma}(t)||}\right|_{eq}$ is an equivalent continuous signal which can replace $\frac{\beta(t)}{2} \frac{\boldsymbol{\sigma}(t)}{||\boldsymbol{\sigma}(t)||}$, and yet still maintain the sliding motion. For further comprehension about the equivalent control concept, please refer to (Utkin, 1992, 2013). Although this concept is an abstraction, its theoretical value can be approximated in real-time by using a low-pass filter

$$\dot{\bar{\boldsymbol{u}}}_{eq}(t) = \mathrm{diag}\left\{\frac{1}{\tau_i}\right\}\left(-\bar{\boldsymbol{u}}_{eq}(t) + \tfrac{\beta(t)}{2}\tfrac{\boldsymbol{\sigma}(t)}{||\boldsymbol{\sigma}(t)||}\right) \qquad (33)$$

where $\bar{\boldsymbol{u}}_{eq} \in \mathbb{R}^n$, and $\tau_i > 0 \in \mathbb{R}$, $i = 1, \ldots, n$ are (small) constants.

Therefore, during the sliding mode, $\boldsymbol{d}(\boldsymbol{\sigma}, t)$ can be estimated in real time through $\bar{\boldsymbol{u}}_{eq}$. Although $\bar{\boldsymbol{u}}_{eq}(t)$ only approximates the equivalent control after the sliding mode takes place, this filtered signal will still be employed in the adaptation scheme during the reaching phase.

Remark 1: Note that, during the sliding mode, the difference between $\bar{\mathbf{u}}_{eq}(t)$ and the real equivalent control, $\mathbf{u}_{eq}(t)$, can be reduced by making τ_i smaller. However, as τ_i becomes smaller, higher frequencies will pass through the filter, making $\bar{\mathbf{u}}_{eq}(t)$ noisier.

Consider the following scalar variable

$$\delta(t) = L(t) - \frac{b}{a\beta_0}||\bar{\boldsymbol{u}}_{eq}(t)|| - \epsilon \qquad (34)$$

where $\epsilon > 0 \in \mathbb{R}$, $a > 0 \in \mathbb{R}$, and $b \geq 1 \in \mathbb{R}$ are design variables and a is chosen such that $a\beta_0 < 1$. The scalar variable b must be chosen such that, for every $\boldsymbol{\sigma}(t) \neq \mathbf{0}$, $b||\boldsymbol{\phi}_2(\boldsymbol{\sigma})|| \geq 1$. Note that, unlike the scheme proposed in (Edwards and Shtessel, 2016), we introduce an additional parameter b into the definition of the auxiliar variable (34) so as to cope with possibly different values for the norm of $\boldsymbol{\phi}_2(\boldsymbol{\sigma})$. Thus, $\delta(t)$ can be modified to allow different choices for $\boldsymbol{\phi}_2(\boldsymbol{\sigma})$, facilitating a possible generalization for a broader class of Super-Twisting based algorithms. As in the original scheme, the other design variables a and ϵ should be interpreted as safety margins ensuring that

$$\frac{b}{a\beta_0}||\bar{\boldsymbol{u}}_{eq}|| + \epsilon \geq \frac{1}{a\beta_0}||\bar{\boldsymbol{u}}_{eq}|| + \epsilon > ||\boldsymbol{u}_{eq}|| \qquad (35)$$

The adaptive function $L(t)$ is defined as

$$L(t) = l(t) + l_0 \qquad (36)$$

where $l_0 > 0 \in \mathbb{R}$ is a constant design parameter, and $l(t)$ is a scalar function with time derivative given by

$$\dot{l}(t) = -\rho(t) sign(\delta(t)), \qquad (37)$$

with $\rho(t) = r_0 + r(t)$ and

$$\dot{r}(t) = \gamma|\delta(t)|, \qquad (38)$$

where $\gamma, r_0 > 0 \in \mathbb{R}$. Given the dual-layer scheme, we can state the second result of this paper.

Theorem 2. Consider the system (1) subject to the input disturbance $\boldsymbol{d}(\boldsymbol{\sigma}, t)$ which satisfies the constraint $||\dot{\boldsymbol{d}}(\boldsymbol{\sigma}, t)|| < a_1$, where the positive constant a_1 is finite but *unknown.* Then, the dual-layer adaptation scheme (33), (34), (36)–(38) ensures $L(t) > ||\boldsymbol{d}(\boldsymbol{\sigma}, t)||$ in finite time.

Proof. The proof follows closely the same steps of the proof of (Edwards and Shtessel, 2016, Proposition 3.2).

Consider the following auxiliary variable

$$e(t) = \frac{bqa_1}{a\beta_0} - r(t), \qquad (39)$$

where $q > 1$ represents a safety margin and is used to ensure that $\left|\frac{d}{dt}||\bar{\boldsymbol{u}}_{eq}(t)||\right| \leq ||\dot{\bar{\boldsymbol{u}}}_{eq}(t)|| < qa_1$. From (38), the time derivative of (39) is given by

$$\dot{e}(t) = -\gamma|\delta(t)| \qquad (40)$$

From (34), it follows that

$$\dot{\delta}(t) = \dot{l}(t) - \frac{b}{a\beta_0}\frac{d}{dt}||\bar{\boldsymbol{u}}_{eq}(t)||. \qquad (41)$$

Given the dynamics of $\delta(t)$ and $e(t)$, the following Lyapunov function candidate will be used to analyze the boundedness of these variables.

$$V(\delta, e) = \frac{\delta^2(t)}{2} + \frac{e^2(t)}{2\gamma} \qquad (42)$$

As in (Edwards and Shtessel, 2016), from (40) and (41), it is possible to conclude that $\delta(t)$ and $e(t)$ are bounded signals. Moreover, since $r(t)$ is also bounded, it can be verified from Barbalat's Lemma (Khalil, 2002) the asymptotic convergence of $\delta(t)$ to zero, ensuring that Assumption 1 is satisfied in finite time.

Remark 2: Theorem 2 imposes only a constraint on the time derivative of the input disturbance. It is important to stress that the adaptive scheme can cope with a class of unbounded disturbances at the expense of allowing unbounded gains as well. This result extends the applicability of the dual-layer scheme proposed in (Edwards and Shtessel, 2016) to a broader class of disturbances/uncertainties. Note that regardless of the unboundedness of $L(t)$, the sliding variables $\boldsymbol{\sigma}(t)$ and $\dot{\boldsymbol{\sigma}}(t)$ remain bounded, according to Theorem 1. On the other hand, if the disturbance is bounded, it is straightforward to conclude that $L(t)$ is also bounded in this case.

Combining Theorems 1 and 2, the main result of this paper is achieved. Note that the sliding mode occurs in finite time in spite of the disturbance term $\boldsymbol{d}(\boldsymbol{\sigma}, t)$. As $\delta(t)$ decreases $L(t)$ becomes a tighter upper-bound for $||\boldsymbol{d}(\boldsymbol{\sigma}, t)||$, keeping the sliding mode and avoiding conservative values for the gains of the Super-Twisting algorithm described in (1).

Remark 3: During the reaching phase there is an interval $[t_a, t_c]$ where $\left|\left|\frac{\boldsymbol{\sigma}(t)}{2||\boldsymbol{\sigma}(t)||}\right|\right| = \frac{1}{2}$ for almost all $t \in [t_a, t_c]$. From (33), and since τ_i are small constants, $\bar{\boldsymbol{u}}_{eq}(t)$ is a high bandwidth low-pass filtered version of $\beta(t)/2$. Moreover, there exists a time interval $[t_b, t_c] \subset [t_a, t_c]$ in which $||\bar{\boldsymbol{u}}_{eq}(t)|| > a\beta(t)/2$. Therefore, for almost all $t \in [t_b, t_c]$, it follows from (2) and (34) that

$$\delta(t) < L(t) - \frac{ab\beta_0 L(t)}{2a\beta_0} - \epsilon$$

From (4), $||\boldsymbol{\phi}_2(\boldsymbol{\sigma})|| = \frac{1}{2}$, $\forall \boldsymbol{\sigma}(t) \neq \mathbf{0}$. Thus, choosing $b = 2$, it is possible to conclude that $\delta(t) < -\epsilon$. From (37) and (38), and since δ is negative for almost all $t \in [t_b, t_c]$ it follows that $\dot{L}(t) = \dot{l}(t) = r(t) + r_0 > 0$. Thus, $L(t)$ is monotonically increasing with an increasing rate greater than r_0. Since, in the worst case the disturbance can grow at a fixed rate, then $L(t)$ will increase to be larger than the disturbance after a finite time.

Since $\delta(t)$ converges to zero assimptotically, the function $r(t)$ is always increasing, which could be a problem. An alternative scheme for practical implementations is presented in (Edwards and Shtessel, 2016).

3. SIMULATION RESULTS

Consider the IEEE 39 bus power system with 10 generators and 39 buses described in (Mei et al., 2011). Using the Kron-reduction technique (Dorfler and Bullo, 2013), the power system can be written as

$$\begin{bmatrix}\dot{\boldsymbol{\theta}}(t)\\ \dot{\boldsymbol{\omega}}(t)\end{bmatrix}=\begin{bmatrix}0 & I\\ \boldsymbol{L_s} & -\boldsymbol{M_g}^{-1}\boldsymbol{D_g}\end{bmatrix}\begin{bmatrix}\boldsymbol{\theta}(t)\\ \boldsymbol{\omega}(t)\end{bmatrix}+\begin{bmatrix}0\\ \boldsymbol{I_{10}}\end{bmatrix}\boldsymbol{u}(t)+\bar{B}_f\boldsymbol{f}(\boldsymbol{\xi},t)$$

$$\dot{\boldsymbol{\xi}}(t)=\bar{\boldsymbol{A}}\boldsymbol{\xi}(t)+\bar{\boldsymbol{B}}\boldsymbol{u}(t)+\bar{\boldsymbol{B}}_f\boldsymbol{f}(\boldsymbol{\xi},t) \tag{43}$$

with $\boldsymbol{\xi}(t)=\left[\boldsymbol{\theta}(t)^T\ \boldsymbol{\omega}(t)^T\right]^T$, $\boldsymbol{L_s}=\boldsymbol{M_g}^{-1}\left(\boldsymbol{L_{gl}}\boldsymbol{L_{ll}}^{-1}\boldsymbol{L_{lg}}-\boldsymbol{L_{gg}}\right)$ and $\boldsymbol{u}(t)=\boldsymbol{M_g}^{-1}\left(\boldsymbol{P_\omega}(t)-\boldsymbol{L_{gl}}\boldsymbol{L_{ll}}^{-1}\boldsymbol{P_\theta}(t)\right)$, where $\boldsymbol{\theta}(t)\in\mathbb{R}^{10}$ and $\boldsymbol{\omega(t)}\in\mathbb{R}^{10}$ denote the generator rotor angles and frequencies, respectively. The vector $\boldsymbol{f}(t)$ describe an unknown attack and $\boldsymbol{u}(t)$ the equivalent input. The line resistance is described by the network susceptance matrix composed by $\boldsymbol{L_{ll}}$, $\boldsymbol{L_{gl}}$, $\boldsymbol{L_{lg}}$ and $\boldsymbol{L_{gg}}$. The matrices $\boldsymbol{M_g}$ and $\boldsymbol{D_g}$ describe the inertial matrix and the damping coefficients, respectively. $\boldsymbol{P_\omega}(t)$ is the known reactive power demand of the buses and $\boldsymbol{P_\theta}(t)$ is the controlled mechanical power input for each generator. The numerical values for the above parameters are described in (Corradini and Cristofaro, 2017).

We consider that the system output is given by

$$\boldsymbol{y}(t)=[\boldsymbol{I_{10}}\ \boldsymbol{I_{10}}]\,\boldsymbol{\xi}(t) \tag{44}$$

Furthermore, the last ten states will be monitored, i.e.

$$\bar{\boldsymbol{B}}_{\boldsymbol{f}}=[\boldsymbol{0}\ \boldsymbol{I_{10}}]^T \tag{45}$$

After a linear change of coordinates $\boldsymbol{x}(t)=\begin{bmatrix}\boldsymbol{I_{10}} & \boldsymbol{0}\\ \boldsymbol{I_{10}} & \boldsymbol{I_{10}}\end{bmatrix}\boldsymbol{\xi}(t)$, the system described by (43), (44), and (45) can be represented as

$$\begin{bmatrix}\dot{\boldsymbol{x}}_{\boldsymbol{1}}(t)\\ \dot{\boldsymbol{x}}_{\boldsymbol{2}}(t)\end{bmatrix}=\begin{bmatrix}\boldsymbol{A_{11}} & \boldsymbol{A_{12}}\\ \boldsymbol{A_{21}} & \boldsymbol{A_{22}}\end{bmatrix}\begin{bmatrix}\boldsymbol{x_1}(t)\\ \boldsymbol{x_2}(t)\end{bmatrix}+\begin{bmatrix}\boldsymbol{B_1}\\ \boldsymbol{B_2}\end{bmatrix}\boldsymbol{u}(t)+\begin{bmatrix}\boldsymbol{0}\\ \boldsymbol{B}\end{bmatrix}\boldsymbol{f}(t)$$
$$\boldsymbol{y}(t)=\boldsymbol{x_2}(t)$$

where $\boldsymbol{A_{11}}$ is a Hurwitz matrix and $\boldsymbol{B}$ is an identity matrix. In order to reconstruct the attack vector $\boldsymbol{f}(t)$, we consider the following state observer

$$\begin{bmatrix}\dot{\hat{\boldsymbol{x}}}_{\boldsymbol{1}}(t)\\ \dot{\hat{\boldsymbol{x}}}_{\boldsymbol{2}}(t)\end{bmatrix}=\begin{bmatrix}\boldsymbol{A_{11}} & \boldsymbol{A_{12}}\\ \boldsymbol{A_{21}} & \boldsymbol{A_{22}}\end{bmatrix}\begin{bmatrix}\hat{\boldsymbol{x}}_{\boldsymbol{1}}(t)\\ \boldsymbol{y}(t)\end{bmatrix}+\begin{bmatrix}\boldsymbol{B_1}\\ \boldsymbol{B_2}\end{bmatrix}\boldsymbol{u}(t)+\begin{bmatrix}\boldsymbol{0}\\ \boldsymbol{B}\end{bmatrix}\hat{\boldsymbol{f}}(t)$$
$$\hat{\boldsymbol{y}}(t)=\hat{\boldsymbol{x}}_{\boldsymbol{2}}(t)$$

Defining the estimation errors as $\boldsymbol{e_1}(t)=\boldsymbol{x_1}(t)-\hat{\boldsymbol{x}}_{\boldsymbol{1}}(t)$, and $\boldsymbol{e_2}(t)=\boldsymbol{x_2}(t)-\hat{\boldsymbol{x}}_{\boldsymbol{2}}(t)$, it follows that

$$\begin{bmatrix}\dot{\boldsymbol{e}}_{\boldsymbol{1}}(t)\\ \dot{\boldsymbol{e}}_{\boldsymbol{2}}(t)\end{bmatrix}=\begin{bmatrix}\boldsymbol{A_{11}}\\ \boldsymbol{A_{21}}\end{bmatrix}\boldsymbol{e_1}(t)+\begin{bmatrix}\boldsymbol{0}\\ \boldsymbol{B}\end{bmatrix}\left(\boldsymbol{f}(t)-\hat{\boldsymbol{f}}(t)\right) \tag{46}$$

Note that $\boldsymbol{e_2}(t)$ is a measurable signal, once $\mathbf{y}(t)-\hat{\boldsymbol{y}}(t)=\boldsymbol{e_2}(t)$. Since $\boldsymbol{A_{11}}$ is Hurwitz, it is possible to conclude that $\boldsymbol{e_1}(t)$ is a bounded signal that converges exponentially to zero. Furthermore, defining $\boldsymbol{\sigma}(t)=\boldsymbol{e_2}(t)$ and

$$\hat{\boldsymbol{f}}(t)=-\boldsymbol{B}^{-1}\left(-\alpha(t)\boldsymbol{\phi}_1(\boldsymbol{\sigma})+\boldsymbol{\Phi}(\boldsymbol{\sigma},t)-\int_{t_0}^{t}\beta(t)\boldsymbol{\phi}_2(\boldsymbol{\sigma})dt\right),$$

the output observation error can be written as (1), with $\boldsymbol{d}(\boldsymbol{\sigma},t)=\boldsymbol{A_{21}}\dot{\boldsymbol{e}}_{\boldsymbol{1}}+\boldsymbol{B}\dot{\boldsymbol{f}}(t)$. Therefore, the sliding mode is achieved in finite time for any disturbance $\boldsymbol{d}(\boldsymbol{\sigma},t)$ that satisfies the constraint $||\dot{\boldsymbol{d}}(\boldsymbol{\sigma},t)||<a_1$, where a_1 is an unknown constant.

Note that after the sliding mode takes place ($\boldsymbol{\sigma}(t)=\dot{\boldsymbol{\sigma}}(t)=\boldsymbol{0}$), $\hat{\boldsymbol{f}}\boldsymbol{(t)}=\boldsymbol{B}^{-1}\boldsymbol{A_{21}}\boldsymbol{e_1}(t)+\boldsymbol{f}(t)$. Since $\boldsymbol{e_1}(t)$ converges to zero exponentially, it follows that $\hat{\boldsymbol{f}}(t)$ also converges exponentially to $\boldsymbol{f}(t)$.

In order to allow a comparison between both approaches, the same simulation parameters considered in (Corradini and Cristofaro, 2017) were chosen here. To simplify the notation, the strategy proposed in (Corradini and Cristofaro, 2017), will be referred here as *Method 2*.

Consider that the power system presented in (43) is under attack by the following attack vector $\boldsymbol{f}(t)=\left[\boldsymbol{0}_{1\times10}\ \ \frac{1}{2}sin(0.2\pi t)\ \ \boldsymbol{0}_{1\times9}\right]^T$. Defining $\kappa=2$, the STA gains are chosen as $\alpha_0=2$ and $\beta_0=3.5$ in order to satisfy (12). The dual-layer parameters are defined as $\tau_i=0.01$, $i=1,...,10$, $r_0=0.1$, $l_0=0.1$, $a=0.24$, $\epsilon=0.01$, and $\gamma=8$.

Note that Method 2 requires the knowledge of an upper-bound for $\boldsymbol{f}(t)$ and its time derivative. Thus, for implementation purposes, it is considered that the constants $\rho_1=0.5$ and $\rho_2=0.1\pi$ are known upper-bounds for $\boldsymbol{f}(t)$ and $\dot{\boldsymbol{f}}(t)$, respectively. It should be emphasized that the proposed strategy only requires that the constraint $||\dot{\boldsymbol{d}}(\boldsymbol{\sigma},t)||<a_1$ presented in Theorem 2 be satisfied.

Considering $\boldsymbol{\sigma}(0)=\left[-0.5\cdot\boldsymbol{1}_{1\times5}\ 0.25\cdot\boldsymbol{1}_{1\times5}\right]^T$ and $\boldsymbol{z}(0)=\boldsymbol{0}$ the simulation results are shown in the following Figures.

From Fig. 1 note that the proposed strategy ensures the 2-SM ($\boldsymbol{\sigma}(t)=\boldsymbol{z}(t)=\boldsymbol{0}$) in finite time and also provides an exact reconstruction of the original attack, as can be observed in Fig. 2. As described in (Corradini and Cristofaro, 2017), Method 2 only ensures the boundedness of the signals $||\boldsymbol{\sigma}(t)||$ and $||\boldsymbol{f}(t)-\hat{\boldsymbol{f}}(t)||$, therefore, the attack reconstruction is not exact (see Fig. 2). Since Method 2 is not based on second-order sliding modes, it does not have a z variable.

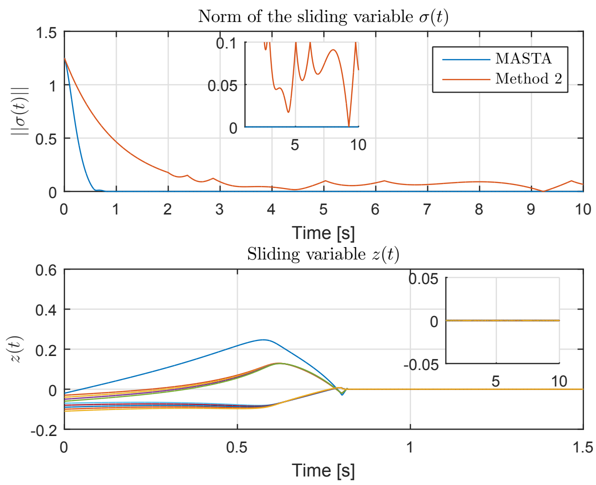

Fig. 1. Sliding variables.

From Fig. 3, the expected behaviors for the adaptive gain $L(t)$ and the Dual-Layer variables $\delta(t)$ and $\rho(t)$ are observed, since $L(t)>||\boldsymbol{d}(\boldsymbol{\sigma},t)||$, $\delta(t)$ converges to zero, and $\rho(t)$ becomes constant.

4. CONCLUSION

In this paper, we have proposed a non-decoupled Multivariable Adaptive Super-Twisting Algorithm (MASTA).

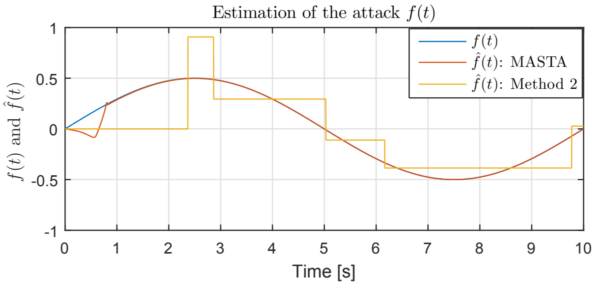

Fig. 2. True $f(t)$ versus estimated $\hat{f}(t)$ state attack using both methods.

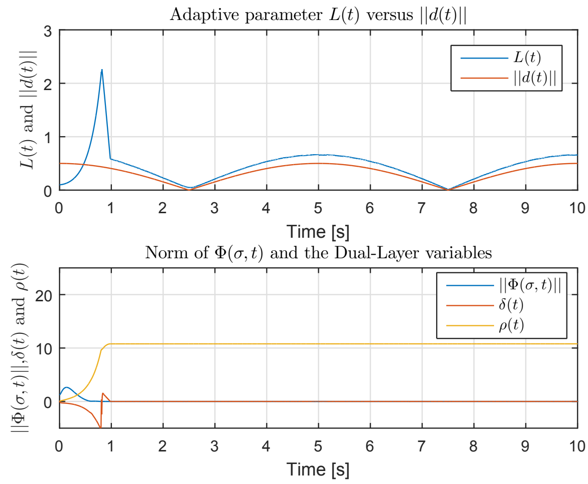

Fig. 3. (a) Adaptive gain $L(t)$ and the disturbance $||\boldsymbol{d}(t)||$. (b)$||\boldsymbol{\Phi}(t, \boldsymbol{\sigma})||$ and the Dual-Layer variables $\delta(t)$, $\rho(t)$.

We have provided a multivariable extension closer to the SISO version presented in (Edwards and Shtessel, 2016), using a generalized formulation. Besides, we have highlighted some key properties that may allow a generalization to a broader class of Super-Twisting based algorithms. Although the filtered signal used to approximate the equivalent control is a vector in the multivariable case, its norm remains a scalar. Thus, the dual-layer scheme, originally proposed for SISO systems, can be used without major modifications if a non-decoupled multivariable approach is considered. The adaptive strategy does not require the knowledge of upper bounds for the matched disturbances, and yet is capable of rejecting bounded disturbances. As an additional contribution, we have shown that the dual-layer scheme can also reject a class of unbounded disturbances if the gains are allowed to be unbounded as well.

REFERENCES

Alwi, H. and Edwards, C. (2013). An adaptive sliding mode differentiator for actuator oscillatory failure case reconstruction. *Automatica*, 49(2), 642–651.

Bartolini, G., Levant, A., Plestan, F., Taleb, M., and Punta, E. (2013). Adaptation of sliding modes. *IMA Journal of Mathematical Control and Information*, 30(3), 285–300.

Bernstein, D.S. (2009). *Matrix mathematics: theory, facts, and formulas*. Princeton university press.

Boiko, I. and Fridman, L. (2005). Analysis of chattering in continuous sliding-mode controllers. *IEEE Transactions on Automatic Control*, 50(9), 1442–1446.

Corradini, M.L. and Cristofaro, A. (2017). Robust detection and reconstruction of state and sensor attacks for cyber-physical systems using sliding modes. *IET Control Theory & Applications*, 11(11), 1756–1766.

Deimling, K. (1992). *Multivalued Differential Equations, de Gruyter Series in Nonlinear Analysis and Applications*. Walter de Gruyter Berlin, Germany.

Dorfler, F. and Bullo, F. (2013). Kron reduction of graphs with applications to electrical networks. *IEEE Transactions on Circuits and Systems I: Regular Papers*, 60(1), 150–163.

Edwards, C. and Shtessel, Y. (2016). Adaptive dual-layer super-twisting control and observation. *International Journal of Control*, 89(9), 1759–1766.

Filippov, A.F. (1964). Differential equations with discontinuous right-hand side. *Amer. Math. Soc. Trans.*, 42, 199–231.

Khalil, H.K. (2002). *Nonlinear systems; 3rd ed.* Prentice-Hall, Upper Saddle River, NJ.

Levant, A. (2003). Higher-order sliding modes, differentiation and output-feedback control. *International Journal of Control*, 76(9-10), 924–941.

Levant, A. (1993). Sliding order and sliding accuracy in sliding mode control. *International journal of control*, 58(6), 1247–1263.

Mei, S., Zhang, X., and Cao, M. (2011). *Power grid complexity*. Springer Science & Business Media.

Moreno, J.A. and Osorio, M. (2008). A lyapunov approach to second-order sliding mode controllers and observers. In *2008 47th IEEE conference on decision and control*, 2856–2861. IEEE.

Plestan, F., Shtessel, Y., Bregeault, V., and Poznyak, A. (2010). New methodologies for adaptive sliding mode control. *International Journal of Control*, 83(9), 1907–1919.

Shtessel, Y., Edwards, C., Fridman, L., and Levant, A. (2014). *Sliding Mode Control and Observation*. Control Engineering. Birkhäuser.

Shtessel, Y., Taleb, M., and Plestan, F. (2012). A novel adaptive-gain supertwisting sliding mode controller: Methodology and application. *Automatica*, 48(5), 759–769.

Utkin, V.I. (1992). *Sliding Modes in Control and Optimization*. Springer-Verlag.

Utkin, V.I. and Poznyak, A.S. (2013). Adaptive sliding mode control with application to super-twist algorithm: Equivalent control method. *Automatica*, 49(1), 39–47.

Utkin, V.I. (2013). *Sliding modes in control and optimization*. Springer Science & Business Media.

Vidal, P.V., Nunes, E.V., and Hsu, L. (2017). Output-feedback multivariable global variable gain super-twisting algorithm. *IEEE Transactions on Automatic Control*, 62(6), 2999–3005.

Zhao, X., Zong, Q., Tian, B., Shao, S., You, M., and Liu, W. (2019). Adaptive multivariable finite-time continuous fault-tolerant control of rigid spacecraft. *International Journal of Robust and Nonlinear Control*, 29(10), 2927–2940.